

The linear and nonlinear inverse Compton scattering between microwaves and electrons in a resonant cavity

Meiyu Si, Shanhong Chen, Manqi Ruan, and Guangyi Tang
Institute of High Energy Physics, Chinese Academy of Sciences, Beijing 100049, China

Yongsheng Huang*
*School of Science, Sun Yat-Sen University, Shenzhen 528406, China and
Institute of High Energy Physics, Chinese Academy of Sciences, Beijing 100049, China*

Xiaofei Lan
Physics and Space Science College, China West Normal University, Nanchong 637009, China

Yuan Chen
National Synchrotron Radiation Laboratory, University of Science and Technology of China, Hefei 230029, China

Xinchou Lou
*Institute of High Energy Physics, Chinese Academy of Sciences, Beijing 100049, China and
State Key Laboratory of Particle Detection and Electronics,
Institute of High Energy Physics, CAS, Beijing 100049, China*

In a free space, the Sunyaev-Zel'dovich (SZ) effect is a small spectral distortion of the cosmic microwave background (CMB) spectrum caused by inverse Compton scattering of microwave background photons from energetic electrons in the plasma. However, the microwave does not propagate with a plane waveform in a resonant cavity, the inverse Compton scattering process is a little different from that in a free space. By taking the Fourier expansion of the microwave field in the cavity, the coefficients of the first-order and the higher-order terms describe the local-space effect on the linear and nonlinear inverse Compton scattering respectively. With our theoretical results, the linear or nonlinear inverse Compton scattering cross section between microwave photons and electrons has important applications on the energy calibration of the extremely energetic electron beam, the sources of the terahertz waves, the extreme ultra-violet (EUV) waves or the mid-infrared beams.

I. INTRODUCTION

The acceleration[1] or deceleration[2] of electrons, or the electromagnetic radiation[3] from electrons occurs in the interaction between electrons and microwaves. And the inverse Compton scattering between microwave photons and electrons does also exist and has played an important role in astrophysics studies[4]. In 1972, the Sunyaev and Zeldovich proposed the SZ effect to describe the inverse Compton scattering between the cosmic microwave background(CMB) photons and the electrons in a galaxy cluster[5]. An unequivocal detection of the Sunyaev-Zeldovich effect has profound cosmological significance[6–11]. For the SZ effect, the CMB photons propagate as the plane waveform in the free space. However, in a resonant cavity, the microwave cannot propagate with a plane waveform. Therefore, in the local space the inverse Compton scattering does be a little different and has not been studied until now.

In this paper, an analytical proposal is given to describe the local-space effect on the inverse Compton scattering between microwaves and electrons in a resonant cavity. With our analytical results, the linear or nonlinear inverse Compton scattering between microwave photons and electrons can be calculated properly in the resonant cavity. As an application of our theoretical results [12, 13], a new microwave-beam inverse Compton scattering method was proposed to measure the beam energy by detecting the Compton edge of the energy distribution of the scattered photons. A cylindrical resonant cavity with TM010 mode is selected to transmit microwaves. Our results on the linear inverse Compton scattering is necessary to calculate the number of the scattered gamma from the inverse Compton scattering between microwave photons and electrons in the resonant cavity. In this case, the effects of the nonlinear Compton scattering are much smaller than that of the linear one and can be ignored. The microwave-electron inverse Compton

* huangysh59@mail.sysu.edu.cn

scattering in a cavity will become a potential competitor of electromagnetic radiations in various frequency bands. For example, a terahertz wave with a frequency of 2 THz can be generated with microwaves scattered by an electron beam with the energy of 5MeV. The linear Compton scattering between a microwave and a 1GeV electron beam can also be an extreme ultra-violet (EUV) wave[14] generator, which is valuable in the field of lithography. The mid-infrared[15] beams with the wavelength of three micrometers can be produced by the inverse Compton scattering between microwaves and an electron beam with the energy of 50MeV. This mid-infrared beams have wide application prospects and play irreplaceable important roles in the fields of remote sensing detection, environmental monitoring, biomedicine, scientific research, and optoelectronic countermeasures[16–20].

II. THEORETICAL MODEL IN A RESONANT CAVITY

In a free space, photons propagate in the form of plane electromagnetic waves. The cylindrical resonant cavity is bounded, the existence of boundary conditions forms a standing wave field in the cavity. The standing wave is stable, there is no movement of the energy in the direction of wave propagation. In the cylindrical cavity, there are three main resonant modes of TM_{mnp} , including TM_{010} , TE_{011} and TE_{111} . In TM_{010} , $m = 0, n = 1, p = 0$, the wave number $K = K_c = \frac{V_{01}}{R} = \frac{2.405}{R}$. The resonance frequency $f = K \cdot c/2\pi$ and resonance wavelength $\lambda = 2\pi/K = 2.613R$, where R is the radius of the cavity. Figure 1 shows the resonant cavity. The electron beam passes through the side wall of the resonant cavity and undergoes inverse Compton scattering with microwave photons. For the TM_{010} mode in the

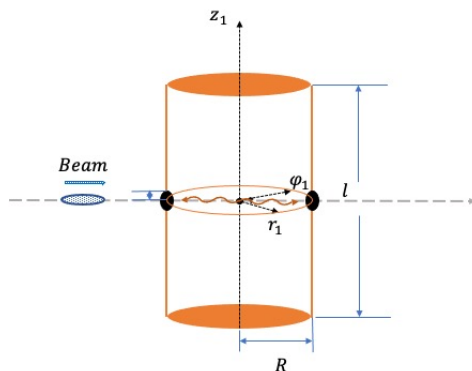


FIG. 1. The electron beam passes through the side wall of a resonant cavity and undergoes inverse Compton scattering with microwave photons. In the cylindrical coordinate system (r_1, φ_1, z_1) , R is the radius of the cavity and l is the length of the cavity. The holes with a radius of 1.5mm are made on the side wall of the cavity to let the electron beam pass through.

cylindrical coordinate system, the electromagnetic field is circularly symmetrical in the cavity[21]. The expression of the electromagnetic field in the resonant cavity is

$$E_{z_1} = E_m J_0(K_c r_1) e^{j\omega t}, \quad (1)$$

$$H_{\varphi_1} = jE_m \frac{1}{\eta} J_1(K_c r_1) e^{j\omega t}, \quad (2)$$

$$E_{r_1} = E_{\varphi_1} = H_{r_1} = H_{z_1} = 0, \quad (3)$$

where $\eta = \sqrt{\frac{\mu_0}{\varepsilon_0}}$, the vacuum permeability $\mu_0 = 4\pi \times 10^{-7} \text{H/m}$, the vacuum dielectric constant $\varepsilon_0 = 8.854188 \times 10^{-12} \text{F/m}$. It is known from Eq.(1), Eq.(2) and Eq.(3) that the electric field only has the longitudinal field in z_1 direction, the magnetic field only has the transverse field in the φ_1 direction. The Poynting vector is the energy flow density vector in the electromagnetic field. The direction of the Poynting vector is radial, which also represents the motion direction of microwave photons[13].

A. Fourier expansion of the microwave field in the cavity

From Eq.(1) and Eq.(2), the electromagnetic field in the resonant cavity is expressed by Bessel function. The zero-order Bessel function $J_0(x)$ in Eq.(1) is an even function. The $J_0(x)$ can be expanded into a cosine series

$\frac{a_0}{2} + \sum_{n=1}^{\infty} a_n \cos nx$. The integral expression of $J_0(x)$ is[22]

$$J_0(x) = \frac{1}{\pi} \int_0^{\pi} \cos(x \sin \theta) d\theta. \quad (4)$$

For $0 < x < \pi$, the coefficients of a_0 and $a_n (n > 1)$ can be written as

$$a_0 = \frac{2}{\pi} \int_0^{\pi} J_0(x) dx = \frac{2}{\pi^2} \int_0^{\pi} \frac{\sin(\pi \sin \theta)}{\sin \theta} d\theta, \quad (5)$$

$$a_n = \frac{2}{\pi} \int_0^{\pi} J_0(x) \cos(nx) dx = \frac{(-1)^n}{\pi^2} \left[\int_0^{\pi} \frac{\sin(\pi \sin \theta)}{n + \sin \theta} d\theta - \int_0^{\pi} \frac{\sin(\pi \sin \theta)}{n - \sin \theta} d\theta \right], \quad (6)$$

where the a_0 and a_n are calculated by numerical integration. Table 1 shows the numerical solution of the coefficients.

n	0	1	2	3	4	5	6	7	...
a_n	0.857862	0.608484	-0.0513979	0.021227	-0.0116605	0.00738341	-0.00509808	0.00373271	...

TABLE I. The numerical solution of the coefficients a_0 and a_n .

The Fourier series expansion of the $J_0(x)$ is

$$J_0(x) = 0.428931 + 0.608484 \cos(1x) - 0.0513979 \cos(2x) + 0.021227 \cos(3x) \\ - 0.0116605 \cos(4x) + 0.00738341 \cos(5x) - 0.00509808 \cos(6x) + 0.00373271 \cos(7x) - \dots. \quad (7)$$

Figure 2 shows the zero-order Bessel function integral expression from Eq.(1) and the series expansion from Eq.(7) in the range of 0 to π . The red dotted line is the Fourier series expansion. The blue line is the integral expression.

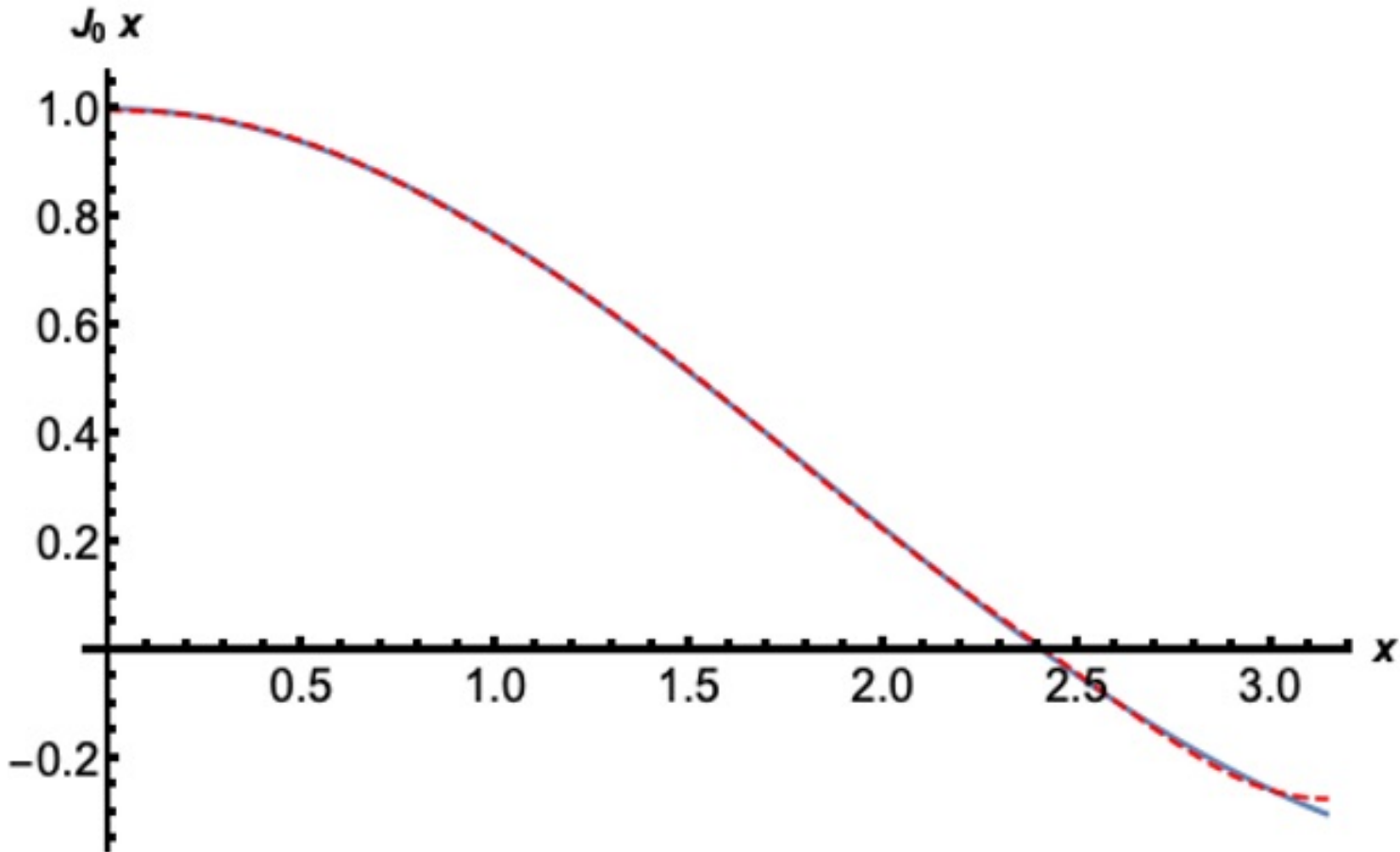


FIG. 2. The zero-order Bessel function integral expression from Eq.(1) and the series expansion from Eq.(7) in the range of 0 to π . The red dotted line is the Fourier series expansion. The blue line is the integral expression.

The first-order Bessel function $J_1(x)$ in Eq.(2) is an odd function. The $J_1(x)$ can be expanded into a sine series $\sum_{n=1}^{\infty} b_n \sin nx$. The integral expression of $J_1(x)$ is[22]

$$J_1(x) = \frac{1}{\pi} \int_0^{\pi} \cos(x \sin \theta - \theta) d\theta. \quad (8)$$

The expansion coefficient of $b_n (n > 1)$ is

$$b_n = \frac{2}{\pi} \int_0^{\pi} J_1(x) \sin(nx) dx = \frac{1}{\pi^2} \left[\int_0^{\pi} \frac{\cos \theta - \cos(n\pi + \pi \sin \theta - \theta)}{n + \sin \theta} d\theta + \int_0^{\pi} \frac{\cos \theta - \cos(n\pi - \pi \sin \theta + \theta)}{n - \sin \theta} d\theta \right]. \quad (9)$$

Table 2 shows the numerical solution of b_n .

n	1	2	3	4	5	6	7	...
b_n	0.608484	-0.102796	0.0636828	-0.046642	0.036917	-0.0305885	0.026129	...

TABLE II. The numerical solution of the coefficients b_n .

The expansion expression of the $J_1(x)$ can be written as

$$J_1(x) = 0.608484 \sin(1x) - 0.102796 \sin(2x) + 0.0636828 \sin(3x) - 0.046642 \sin(4x) + 0.036917 \sin(5x) - 0.0305885 \sin(6x) + 0.026129 \sin(7x) - \dots. \quad (10)$$

Figure 3 shows the integral expression of $J_1(x)$ from Eq.(8) and the series expansion from Eq.(10).

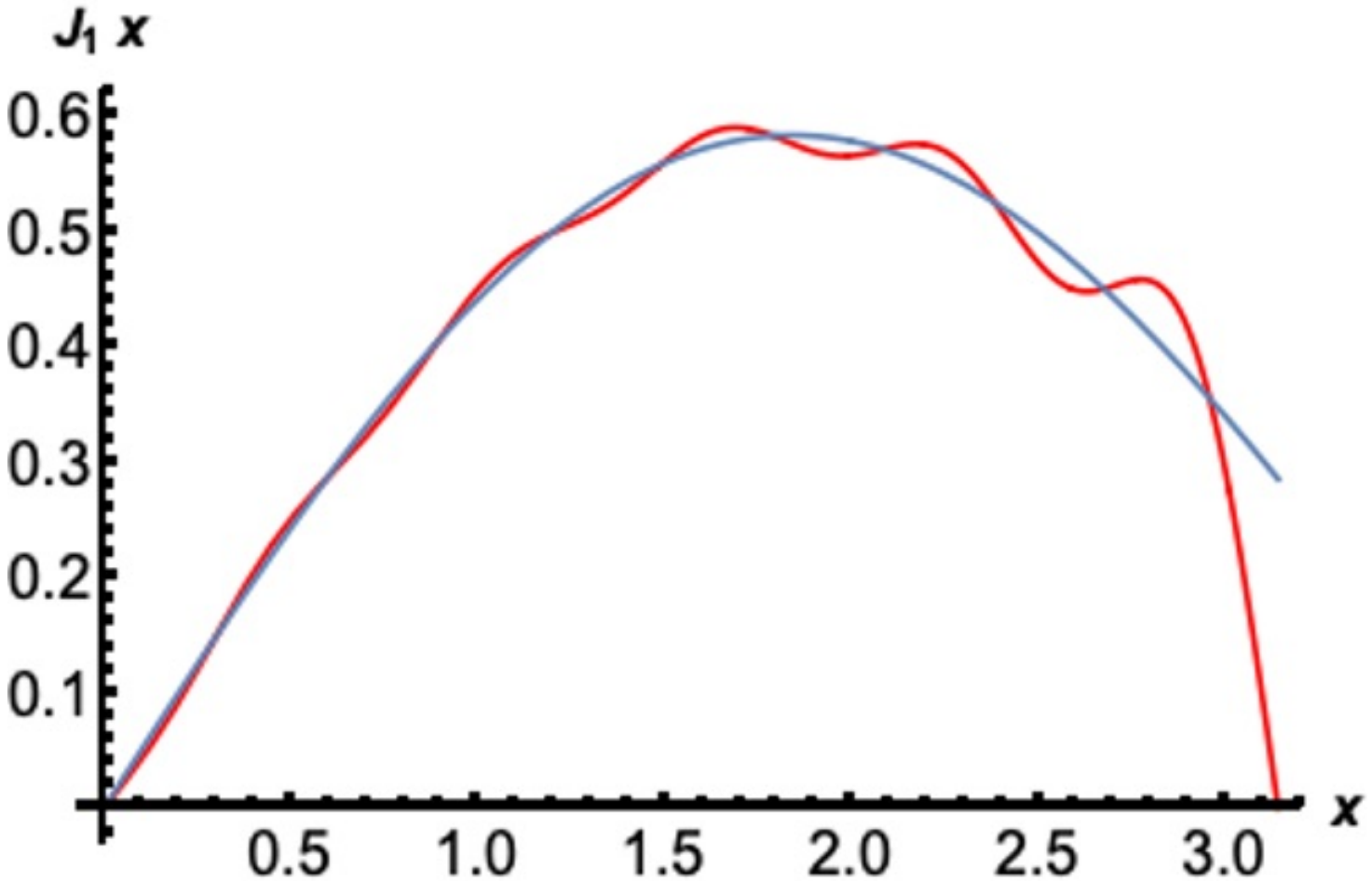


FIG. 3. The integral expression of $J_1(x)$ from Eq.(8) and the series expansion from Eq.(10) in the range of 0 to π . The red line is the Fourier series expansion. The blue line is the integral expression of $J_1(x)$.

The electromagnetic field in the resonant cavity can be expanded into the superposition of multiple plane waves. The zero-order, first-order, and higher-order terms after series expansion are analyzed respectively. Expanding the Bessel function, the zero-order term $J_0(K_c r_1)^{(0)} = 0.428931$, $J_1(K_c r_1)^{(0)} = 0$. According to the Eq.(1) and Eq.(2), the $E_{z_1}^{(0)} = 0.428931 E_m e^{j\omega t}$, $H_{\varphi_1}^{(0)} = 0$. The electric field is a constant. From Eq.(7), the first-order term of Bessel function is $J_0(K_c r_1)^{(1)} = 0.608484 \cos(K_c r_1)$. Similarly, from Eq.(10), $J_1(K_c r_1)^{(1)} = 0.608484 \sin(K_c r_1)$. The exponential expression is

$$J_0(K_c r_1)^{(1)} = 0.608484 e^{-j K_c r_1}, \quad (11)$$

$$J_1(K_c r_1)^{(1)} = -0.608484 e^{-j(\frac{\pi}{2} + K_c r_1)}. \quad (12)$$

Substituting the Eq.(11) and Eq.(12) into Eq.(1) and Eq.(2), and set the coefficient of Bessel function $F_{(TM_{010})}^{(1)} = 0.608484$. The electromagnetic field of the first-order term is

$$E_{z_1}^{(1)} = F_{(TM_{010})}^{(1)} E_m e^{j(\omega t - K_c r_1)}, \quad (13)$$

$$H_{\varphi_1}^{(1)} = -F_{(TM_{010})}^{(1)} E_m \frac{1}{\eta} e^{j(\omega t - K_c r_1)}. \quad (14)$$

For $\vec{E} = -\frac{\partial \vec{A}}{\partial t}$, the vector \vec{A} is given by

$$A_{z_1}^{(1)} = -F_{(TM_{010})}^{(1)} E_m \frac{1}{\omega j} e^{j(\omega t - K_c r_1)}. \quad (15)$$

$B_{\varphi_1} = -\nabla_{r_1} \times A_{z_1}$, $H'_{\varphi_1} = B_{\varphi_1} / \mu_0 = \frac{1}{\mu_0} (-\nabla_{r_1} \times A_{z_1})$. The dispersion relation $\omega = K_c c$ at the first-order term. The H'_{φ_1} is

$$H'_{\varphi_1} = -\frac{1}{\mu_0} \left(-F_{(TM_{010})}^{(1)} E_m \frac{1}{\omega j} e^{j(\omega t - K_c r_1)} \right) \cdot (-j K_c) = -\frac{1}{\mu_0 c} F_{(TM_{010})}^{(1)} E_m e^{j(\omega t - K_c r_1)}. \quad (16)$$

For the relationship of $\mu_0 \varepsilon_0 = \frac{1}{c^2}$, $\frac{1}{\mu_0 c} = \sqrt{\frac{\varepsilon_0}{\mu_0}} = \frac{1}{\eta}$. Simplify Eq.(16) to be

$$H'_{\varphi_1} = -F_{(TM_{010})}^{(1)} E_m \frac{1}{\eta} e^{j(\omega t - K_c r_1)} = H_{\varphi_1}^{(1)}, \quad (17)$$

where the Eq.(17) is equal to Eq.(14). The expansion of the first-order electromagnetic field is satisfying Maxwell's equations. For the $E_{z_1}^{(1)}$ and $H_{\varphi_1}^{(1)}$, the frequency and wavelength are ω , $\frac{2\pi}{K_c}$ respectively. The energy and momentum are $\hbar\omega$ and $\hbar\vec{K}_c$. The expression of $\omega^2 = c^2 K_c^2$ is the on-shell condition and the vacuum dispersion relationship. The linear inverse Compton scattering can occur between electrons and microwave photons. For higher-order terms, the expansion of the Bessel function is

$$J_0(K_c r_1)^{(2)+(3)+(4)+(5)+\dots} = -0.0513979 \cos(2K_c r_1) + 0.0212276 \cos(3K_c r_1) \\ -0.0116605 \cos(4K_c r_1) + 0.00738341 \cos(5K_c r_1) + \dots, \quad (18)$$

$$J_1(K_c r_1)^{(2)+(3)+(4)+(5)+\dots} = -0.102796 \sin(2K_c r_1) + 0.0636828 \sin(3K_c r_1) \\ -0.046642 \sin(4K_c r_1) + 0.036917 \sin(5K_c r_1) + \dots, \quad (19)$$

The wave number is nK_c ($n > 1$), the resonant angular frequency ω remains unchanged. The energy of the photon is $\hbar\omega$, the momentum is $\hbar n \vec{K}_c$, $\omega^2 - (c \cdot n K_c)^2 < 0$, the photon is a virtual photon particle. The nonlinear inverse Compton scattering occurs between the virtual photons and electrons.

B. The cross section of the linear inverse Compton scattering

It is necessary to calculate the cross section of inverse Compton scattering between microwave photons and electrons in the resonant cavity. According to the expansion of the electromagnetic field in the cavity, the coefficients of the higher-order terms are much smaller than those of the first-order term. Therefore, the higher-order terms correspond to the nonlinear inverse Compton scattering which is much weaker than the linear one. The cross section of the inverse Compton scattering in a free space is[23]

$$d\sigma_0 = \frac{r_e^2}{\kappa^2(1+u)^3} \left\{ \kappa[1 + (1+u)^2] - 4\frac{u}{\kappa}(1+u)(\kappa-u) \right\} dud\varphi, \quad (20)$$

where $\kappa(\alpha) = 4\frac{\omega_0\varepsilon_0}{(mc^2)^2}\sin^2(\frac{\alpha}{2})$, the dimensionless constant $u = \frac{\omega}{\varepsilon_0 - \omega}$. The ε_0 and ω_0 is the initial energy of electrons and microwave photons respectively. The ε and ω is the energy of scattered electrons and photons respectively. The α is the collision angle between initial electron and initial photon. According to the first-order coefficients in electric and magnetic fields, the inverse Compton scattering cross section in the cavity has a coefficient $|F_{(TM010)}^{(1)}|^2$. The differential scattering cross section in the resonant cavity is

$$d\sigma_0 = |F_{(TM010)}^{(1)}|^2 \cdot \frac{r_e^2}{\kappa^2(1+u)^3} \left\{ \kappa[1 + (1+u)^2] - 4\frac{u}{\kappa}(1+u)(\kappa-u) \right\} dud\varphi, \quad (21)$$

for $0 < \varphi < 2\pi$, the relationship between the differential cross section and the energy of the scattered photons ω can be written as

$$\frac{d\sigma_0}{d\omega} = |F_{(TM010)}^{(1)}|^2 \cdot 2\pi \frac{r_e^2}{\kappa^2(1+u)^3} \frac{\varepsilon_0}{(\varepsilon_0 - \omega)^2} \left\{ \kappa[1 + (1+u)^2] - 4\frac{u}{\kappa}(1+u)(\kappa-u) \right\}. \quad (22)$$

The microwaves with a wavelength of 3.04cm collide head-to-head with 120GeV electrons on CEPC. According to the inverse Compton scattering process[13], the maximum energy of scattered photons is 9 MeV. From the Eq.(22), the relationship between the Compton differential scattering cross section and the energy of the scattered photons can be obtained in Figure 4. The inverse Compton scattering differential cross section of electrons and microwave photons is about 0.04 barn.

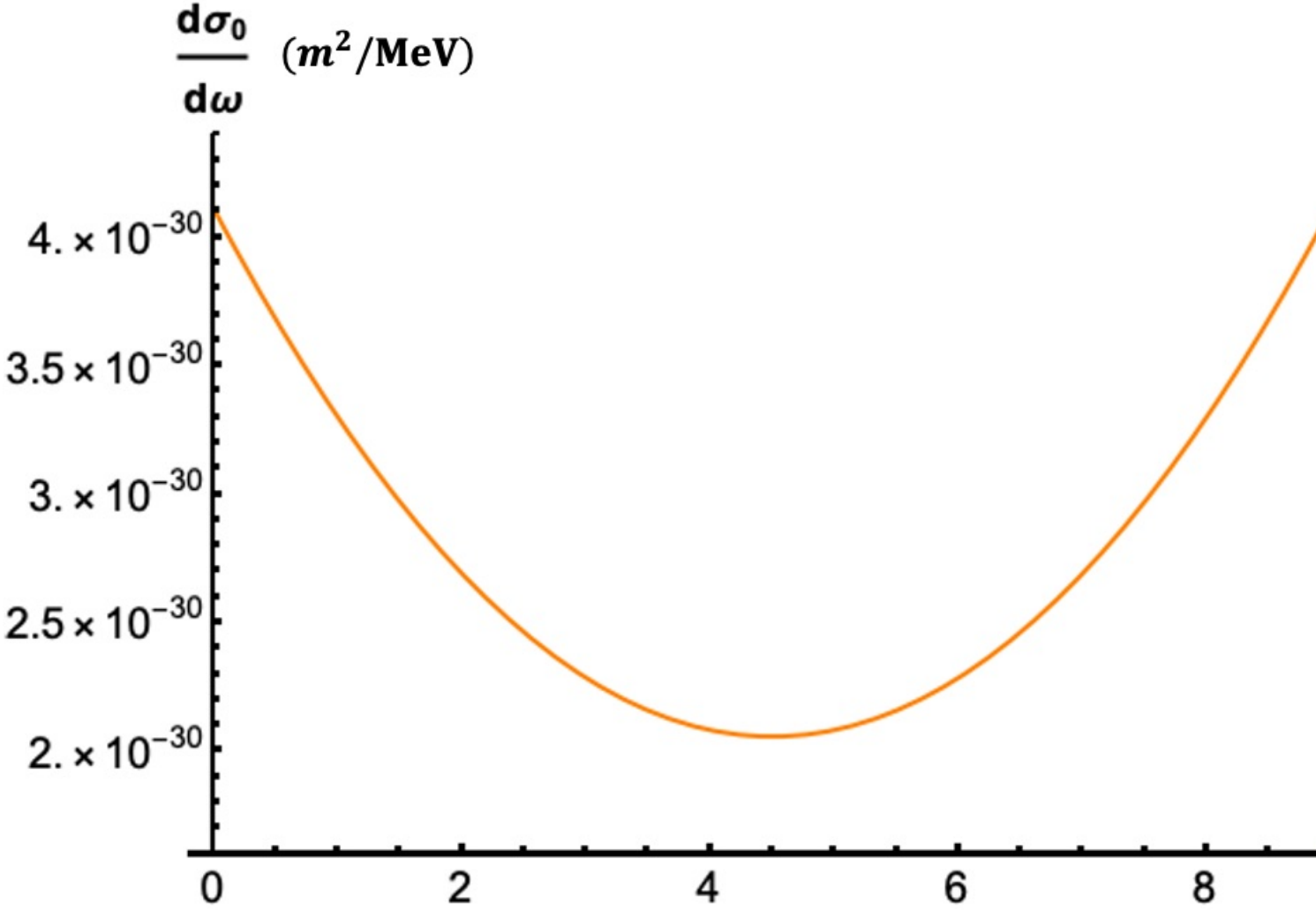


FIG. 4. For the microwaves with a wavelength of 3.04cm collide head-to-head with 120GeV electrons on CEPC, the maximum energy of scattered photons is 9MeV. The relationship between the Compton differential scattering cross section and the energy of scattered photons in a local-space is obtained by Eq.(22). The differential cross section of electrons and microwave photons is about 0.04 barn.

C. The cross section of the nonlinear inverse Compton scattering

For the microwaves with a wavelength of 3.04cm, the initial microwave photon is a virtual photon particle in higher-order terms from Eq.(18) and Eq.(19). The nonlinear inverse Compton scattering occurs between the virtual photons and electrons. From the conservation of energy and momentum, it can be found that the higher-energy scattered photons will emerge. For $n = 2$, the maximum energy of scattered photons is 14MeV; $n = 3$, the maximum energy of scattered photons is 18MeV; $n = 4$, the maximum energy of scattered photons is 23MeV; $n = 5$, the maximum energy of scattered photons is 27MeV, and so on. The expansion coefficients of the higher-order terms ($n=2, n=3, n=4, n=5$) from Table I and Table II are substituted into the Eq.(20) respectively. For example, according to the second-order electric and magnetic field coefficients, the nonlinear inverse Compton scattering cross section in the cavity has a coefficient $|(-0.0513979) \times (-0.102796)|$. Therefore, the differential cross sections corresponding to the maximum energy of the scattering photons are obtained in figure 5. The first point in figure 5 is the differential cross section of the linear inverse Compton scattering.

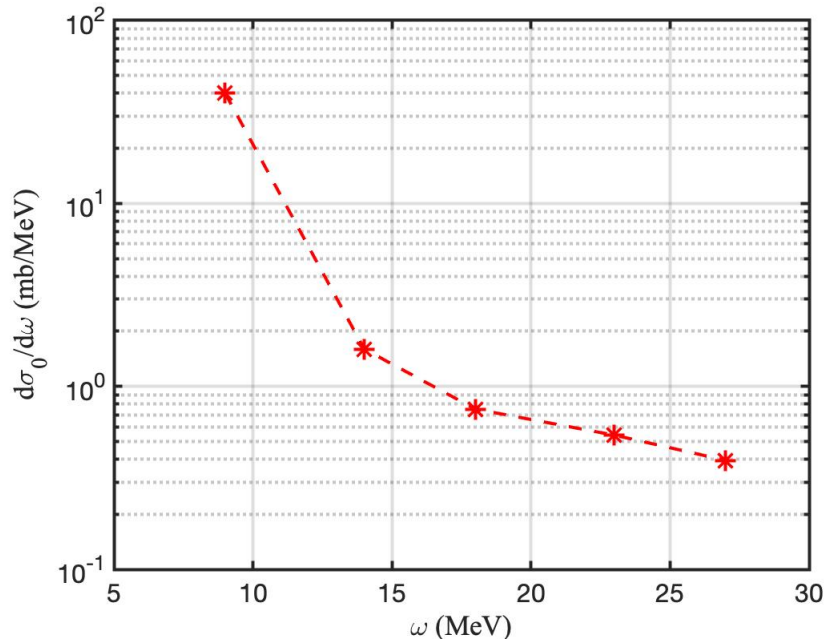


FIG. 5. The differential cross sections of nonlinear Compton scattering between microwaves photons with a wavelength of 3.04cm and 120GeV electrons in the head-on-head collisional mode. According to the conservation of energy and momentum, the maximum energy of linear Compton scattered photons is 9MeV, and the high-energy scattered photons correspond to the nonlinear inverse Compton scattering. The maximum gamma energy of the nonlinear Compton scattering is $\omega = 14\text{MeV}$, $\omega = 18\text{MeV}$, $\omega = 23\text{MeV}$, $\omega = 27\text{MeV}$, corresponding to the nonlinear order 2, 3, 4, 5, respectively.

III. SUMMARY

In this paper, the inverse Compton scattering between microwave photons and electrons in the local-space is calculated theoretically. In a resonant cavity, the electromagnetic field is composed of Bessel functions. By Fourier expansion of Bessel functions, the standing wave field formed in the cavity can be expanded into the superposition of plane waves. According to the theoretical results, the linear inverse Compton scattering of microwave photons and electrons is decided by the first-order term. The nonlinear inverse Compton scattering comes from a high-order frequency virtual photon scattered by high energy electrons. According to the coefficients of each term of the expansion, the differential cross sections of microwave photons and electrons in the local-space can be calculated. The linear inverse Compton scattering between the microwaves and the high energy electron beam can be applied to the simplification of the energy calibration of the electron beam with the energy of tens of or hundreds of GeV[13]. The higher the order of the nonlinear inverse Compton scattering, the smaller the corresponding differential cross section. The linear or nonlinear inverse Compton scattering cross section between microwave photons and electrons has important potential applications on the sources of the terahertz waves, the extreme ultra-violet (EUV) waves or the mid-infrared beams and so on.

IV. ACKNOWLEDGMENT

This work is supported in part by National Natural Science Foundation of China (11655003); Innovation Project of IHEP (542017IHEPZZBS11820, 542018IHEPZZBS12427); the CAS Center for Excellence in Particle Physics (CCEPP); IHEP Innovation Grant (Y4545170Y2); Chinese Academy of Science Focused Science Grant (QYZDY-SSW-SLH002); Chinese Academy of Science Special Grant for Large Scientific Projects (113111KYSB20170005); National 1000 Talents Program of China; the National Key Research and Development Program of China (No.2018YFA0404300).

V. DATA AVAILABILITY

The data that support the findings of this study are available from the corresponding author upon reasonable request.

-
- [1] Davis, T. J. , et al. "High power X-Band microwave amplifiers and their application for particle acceleration." International Conference on High-power Particle Beams IEEE, 1992.
 - [2] Savilov, and V. A. . "Regime of trapping and adiabatic deceleration of electrons in a sectioned electron RF generator." Plasma Science IEEE Transactions on 26.1(1998):36-40.
 - [3] Spero, D. M. , B. J. Eastlund , and M. G. Urv . "Method and apparatus for generating electromagnetic radiation." WO, US3911318 A. 1975.
 - [4] Boughn, S. P.. "Search for correlated large-scale structure in the cosmic x ray and cosmic microwave backgrounds." (1993).
 - [5] Wayne, Dodelson, and Scott. "COSMIC MICROWAVE BACKGROUND ANISOTROPIES.", Annual Review of Astronomy and Astrophysics (2002).
 - [6] M. rknshaw, S.F. u, and H. Hardck†. "The Sunyaev–Zeldovich effect towards three clusters of galaxies." Nature (1984).
 - [7] Gunn, J. E. , M. J. Rees , and M. S. Longair . Observational cosmology. Cambridge University Press, 1978.
 - [8] White, S. D. M., Silk, J. I. Astrophys. J. Lett. 226, L103-106 (1978).
 - [9] Birkinshaw, M. Mon. Not. R. astr. Soc. 187, 847-862 (1979).
 - [10] Fabbri, R., Melchiorri, F. Mencaraglia, F., Natale, V. Astr. Astrophys. 74, L20-24 (1979).
 - [11] Cavaliere, A., Danese, L., De Zotti, G. Astr. Astrophys. 75, 322-325 (1979).
 - [12] K.Y. Zhao, "Microwave principle and technology.", Higher Education Press(2006).
 - [13] M.Y. Si, Y.S. Huang et al., arXiv:2108.09707 [hep-ex] (2021).
 - [14] T Molde. "Ultraviolet Waves. " South Australian Science Teachers Journal (1973):N/A.
 - [15] Daly, J. G. . "Mid-infrared laser applications." Proceedings of SPIE - The International Society for Optical Engineering 1419(1991):94-99.
 - [16] Fuchs, F. , et al. "Remote sensing of explosives using mid-infrared quantum cascade lasers." Proceedings of SPIE - The International Society for Optical Engineering 6739.21(2007):1290 - 1292.
 - [17] Nedeljkovi, M. , et al. "Mid-infrared silicon photonic devices for sensing applications." 5th EOS Topical Meeting on Optical Microsystems International Society for Optics and Photonics, 2013.
 - [18] Tittel, F. K. , et al. "Mid-infrared Laser Based Gas Sensor Technologies for Environmental Monitoring, Medical Diagnostics, Industrial and Security Applications." Springer Netherlands (2014).
 - [19] Hudson, D. D. , et al. "Toward all-fiber supercontinuum spanning the mid-infrared." Optica 4.10(2017):1163.
 - [20] Ebrahim-Zadeh, M. , and I. T. Sorokina . "Mid-Infrared Coherent Sources and Applications." NATO Science for Peace and Security Series B: Physics and Biophysics (2008):626.
 - [21] H.G. Tang, C.Q. Tian, "Microwave Technology principle and Application analysis.",China Science and Technology Investment 000.036(2012):156-156.
 - [22] C.S. Wu,"Special topics on mathematical physics methods: mathematical equations and special functions.",Peking University Press, 2012.
 - [23] N. Muchnoi, arXiv:1803.09595 [physics.ins-det] (2018).